Impact of Substrates on the Electrical Properties of Thin Chromium Films*

Impacto de los sustratos sobre las propiedades eléctricas de las películas delgadas de cromo

Date received: 8 October 2018 | Date approved: 14 March 2019 | Date published: 6 December 2019

Shiva. L. Udachan [a]
Rani Channamma University, India
ORCID: 0000-0002-0810-8353

Narasimha H. Ayachit
Rani Channamma University, India
ORCID: 0000-0002-5463-2586

Lingappa A. Udachan
S. S. Tegnoor Degree College, India
ORCID: 0000-0001-9028-9837

* Research article

[a] Corresponding author. E-mail: ulingappa@gmail.com

DOI: https://doi.org/10.11144/Javeriana.iyu23-2.isep

How to cite this article:
S. L. Udachan, N. H. Ayachit, and L. A. Udachan, "Impact of substrates on the electrical properties of thin chromium films," *Ing. Univ.*, vol. 23, no. 2, 2019. https://doi.org/10.11144/Javeriana.iyu23-2.isep

Abstract

Objective: We studied the impact of substrates on the electrical properties of thin chromium films. Substrates may serve many purposes, such as to define orientation, to conduct electrical current in vertical devices, as a gate in transistors, etc. The thickness range of the chromium films grown on both substrates was 3.5-70 nm. *Methods and materials*: We used Fuchs-Sondheimer (F-S) and Mayadas-Shatzkes (M-S) theories to analyze electrical resistivity data for chromium (Cr) films grown on both substrates simultaneously by thermal evaporation in vacuum, under identical deposition conditions. *Results and discussion:* The infinitely thick film resistivity (ρ_0), conduction electron mean free path (l), specularity parameter (p), scattering power of the grain boundary (α') and grain boundary reflection coefficient (R') were found to depend upon the nature of the substrate and the binding force between them and evaporated chromium atoms. The growth and microstructure of the chromium films were examined using atomic force microscopy (AFM) and scanning electron microscopy (SEM). *Conclusions:* Our experimental data exactly fits with the M-S theory in the entire thickness range grown for the chromium films deposited on both the substrates. Examination of film structure by SEM indicated that the films consist of grains of relatively pure chromium of different sizes, and depends upon deposition conditions and parameters, which are important factors that dictate the structural properties of the films.

Keywords: Atomic force microscopy, grain boundary reflection coefficient, scanning electron microscopy, substrates, resistivity, thin chromium films.

Resumen

Objetivo: Estudiamos el impacto de los sustratos sobre las propiedades eléctricas de las películas delgadas de cromo. Los sustratos pueden servir para muchos propósitos, tales como definir la orientación, conducir corriente eléctrica en dispositivos verticales, actuar como entrada en los transistores, etc. El rango de grosor de las películas de cromo depositadas en ambos sustratos fue (3,5-70) nm. *Métodos y materiales*: Usamos las teorías de Fuchs-Sondheimer (F-S) y de Mayadas-Shatzkes (M-S) para analizar datos de resistividad eléctrica para películas de cromo (Cr) depositadas en ambos sustratos simultáneamente mediante evaporación térmica en el vacío, bajo condiciones de deposición idénticas. *Resultados y discusión*: Se encontró que la resistividad de la película infinitamente gruesa (ρ0), la ruta libre media de electrones de conducción (l), el parámetro de especularidad (p), el poder de dispersión del borde grano (α') y el coeficiente de reflexión del borde de grano (R') dependen de la naturaleza del sustrato y la fuerza de enlace entre ellos y los átomos de cromo evaporados. El crecimiento y la microestructura de las películas de cromo fueron examinados usando microscopía de fuerza atómica (AFM) y microscopía electrónica de barrido (SEM). *Conclusiones*: Nuestros datos experimentales se corresponden con exactitud con la teoría M-S en todo el rango de grosor que creció en las películas de cromo depositadas en ambos sustratos. El examen de la estructura de las películas mediante SEM indicó que las películas constan de granos de cromo relativamente puro de diferentes tamaños y que depende de las condiciones y parámetros de deposición, que son factores importantes que determinan las propiedades estructurales de las películas.

Palabras clave: microscopía de fuerza atómica, coeficiente de reflexión del borde de grano, microscopía electrónica de barrido, sustratos, resistividad, películas delgadas de cromo.

Introduction

Thin chromium films have found many applications, for example, chromium was the first metal to be investigated as a thin film resistor material and has been used in photo-masks, integrated circuits, optical beam splitters, semi-reflective coatings and magnetic recording disks. The substrates serve as mechanical supports but they will also act as insulating materials for electrical measurements.

The deposition parameters, include substrate temperature [1]–[4], substrate materials [5]–[7], deposition pressure, deposition rate [8], and application of DC fields [9] during the formation of the film, play vital roles in the nucleation, growth and other characteristics of films. The tailoring of deposition parameters is the main issue for their application in electronics.

The goal of the present work is to investigate the impact of substrate material on the microstructure, electron mean free path, specularity parameter, scattering power of the grain boundary, grain boundary reflection coefficient and resistivity of infinitely thick chromium films because of their smooth surface and dielectric nature.

The microstructures of the chromium films were investigated via AFM & SEM images. Initial EDS analysis usually involves the generation of an X-ray spectrum from the entire scan area of the material under investigation; the material was identified as chromium.

Methods and Materials

Theoretical Section

Conduction Electron Mean Free Path (l) in Bulk Chromium

The reason for selecting this thickness range (3.5-70 nm) is that we first estimated the conduction electron mean free path value in bulk chromium by the electrical conductivity (σ) equation [10],

$$\sigma = \frac{ne^2\tau}{m} \tag{1}$$

where

n = concentration of electrons/m^3

e = electronic charge

τ = relaxation time

m = mass of one electron and

$\tau = \frac{l}{V_F}$

l = conduction electron means free path

V_F = velocity of electrons at the Fermi surface

The mean free path of conduction electrons was calculated from equation 1, to be 15.2 nm. Hence, we selected the thickness range around this value.

Electrical Resistivity in Thin Films

Fuchs-Sondheimer (F-S) Theory

The electrical response of metal thin films with a thickness approaching, the range of the electron mean free path is highly affected by electronic scattering with interfaces and defects. Fuchs performed a detailed analysis of the size effect by solving, Boltzmann's transport equation with appropriate boundary conditions [11]. He obtained an expression for the electrical resistivity ratio [12] as

$$\frac{\rho_0}{\rho} = \frac{\sigma}{\sigma_0} = 1 - \frac{3}{4}\left(\lambda - \frac{\lambda^3}{12}\right) E_i(-\lambda) - \frac{3}{8\lambda}\left(1 - e^{-\lambda}\right) - \left(\frac{5}{8} + \frac{\lambda}{16} - \frac{\lambda^2}{16}\right) e^{-\lambda} \quad (2)$$

where

$-E_i(-\lambda) = \int_{\lambda}^{\infty} \left(\frac{e^{-t}}{t}\right) dt$ and

σ_0 = conductivity of an infinitely thick film

σ = conductivity of an infinitely thin film

$\lambda = \frac{t}{l} = \frac{\text{film thickness}}{\text{conduction electron mean free path}}$

Equation 2 can be approximated for convenience as

$$\rho = \rho_0 \left[1 + \frac{3}{8\lambda}\right], \lambda > 0.1 \quad (3)$$

where ρ and ρ_0 are the electrical resistivity of the film and infinitely thick film respectively. There is good agreement between this equation and the exact equation over a wide range of λ values.

However, this consideration is for total scattering, therefore a sophisticated theory was developed by Sondheimer [13] to measure the deviation of size effect from the bulk behavior due to the size effect.

He introduced a specularity parameter (p), which represents the fraction of electrons, scattered from the film surface, p has a value ranging from 0 to 1. For complete specular reflection $p = 1$, and the conductivity is not thickness dependent in this case. For total diffuse scattering, $p = 0$; assuming that a fraction p of electrons is specularly scattered at the surface of the film and the remaining fraction is scattered diffusely, equation 3 can be written as

$$\rho = \rho_0 \left[1 + \frac{3(1-p)}{8\lambda}\right], \lambda > 0.1 \quad (4)$$

Multiplying both sides by *t*, we obtain $\rho t = \rho_0 t\,[1 + \frac{3(1-p)}{8\lambda}]$

Substituting $\lambda = t/l$, the equation reduces to $\rho t = \rho_0 t + \frac{3\,l\,(1-p)}{8}\ \rho_0$

This is a linear between ρ x *t* and *t*, with slope ρ_0 and an intercept on the $(\rho \text{ x } t)$ axis as $\frac{3\,l\,(1-p)}{8}\ \rho_0$.

Equation 4 is popularly known as the F-S equation.

Mayadas-Shatzkes (M-S) Theory

Thin films often have island or grain like structures and are discontinuous. When these grains or islands have dimensions on the order of the conduction electron mean free path, the scattering at the grain boundaries leads to a very high resistivity. To estimate the contribution of grain boundary scattering to the total film resistivity, Mayadas-Shatzkes [14] made the important assumptions that the grain boundary potential could be represented by the Diracδ function along with

(1) Isotropic background scattering,
(2) Surface scattering and
(3) Grain boundary scattering.

Mayadas-Shatzkes solved Boltzmann's transport equation using the above model, imposing necessary boundary conditions. They finally arrived at the relation,

$$\frac{\rho_0}{\rho_g} = 3\left[\frac{1}{3} - \frac{1}{2(\alpha')} + \alpha'\right] \text{ for small } \alpha' \qquad (5)$$

where

ρ_o/ρ_g is the ratio of background resistivity (ρ_o) to grain boundary background resistivity ρ_g,
α' is the scattering power of grain boundaries and is given by,

$$\alpha' = \frac{l\,R'}{d\,(1-R')} \qquad (6)$$

where

d is the grain diameter,
and *R'* is the grain boundary reflection coefficient,

With the grain boundary scattering consideration, the total resistivity of the film becomes

$$\rho = \rho_0 \left[1 + \frac{3(1-p)}{8\lambda} + \frac{3}{2}\alpha'\right] \quad (7)$$

The third term on the right hand side (RHS) of equation 7 is the contribution to the total resistivity (ρ) from grain boundary scattering.

Experimental Technique Section

AFM Measurements

Atomic force microscopy (AFM) is a method used to see surfaces, in full three-dimensional detail down to the nanometer scale. The method applies to hard and soft synthetic materials, thin films and biological structures irrespective opaqueness or conductivity. The AFM instrument used in the present investigation and its specifications are given below: Model No: Nanosurf Easyscan 2 FLEX AFM
Serial No: 38-12-178

Microfabricated cantilever
Length: 450 µm (micro meter)
Width: 45 µm
Thickness: 1.5 µm
AFM tip height: 1.2 µm

SEM and EDS Measurements

Nucleation and cluster formations from vapor phase involves the condensation of the vapor stream directly to the solid phase on the surface of the substrates. The condensation of vapor atoms/molecules on an inert solid substrate takes place from a supersaturated conditions. Qualitative and quantitative atomic information for the specimen can be supplied by EDS analysis.

The chromium films grown onto substrates were examined using a scanning electron microscope. A sample of suitable size was taken, it was ground, polished and then etched using suitable etchants, such as a gold coating. Sample preparation for EDS was the same as that for SEM analysis. The SEM instrument used in the present investigation and its specifications are given below:

SEM Type: KYKY-EM3200

Target:
Resolution 6.0 nm guaranteed (Tungsten filaments)
Magnification 15,000X-2.50.000X
Electron optical system
Electron gun: tungsten emitter
Accelerating voltage: 0-30kV

Thermal Evaporation under Vacuum

(a) Experimental Method

The vacuum coating unit used in the present investigation to grow thin films of chromium was a ‘‘Hind High Vacuum Coating Unit, Model 12A4D”. The film thickness was controlled and measured by means of an in-built quartz crystal digital thickness monitor (Model DTM-101). Chromium of purity 99.99 % was evaporated from a tungsten basket at a rate of 0.5 nm/s under a vacuum of 2×10^{-6} Torr onto cleaned soda lime glass and quartz substrates simultaneously at room temperature (23 ºC). The distance between the substrates and the evaporation source was approximately 0.20 m.

(b) Substrate Cleaning Technique

The substrates were first cleaned in chromic acid and then ultrasonically cleaned. That is, the substrates were suspended in an ultrasonic wave generator tank, containing detergent water and agitated with ultrasonic frequency.

Finally, the substrates were rinsed in distilled water, dried and then mounted on a substrate holderplate and kept in the vacuum chamber. Before further deposition of the Cr films, again all the substrates were cleaned by ionic bombardment technique in the vacuum chamber. Prior to deposition of the film, the system was thoroughly degassed.

(c) Measurement of Resistance

For the resistance measurements, indium contacts were placed on the substrates with copper wires for connection purposes. Before deposition, it was inserted into the vacuum chamber and prepared for condensation. The material used in the electrodes to measure the resistance was indium, and the conduction current was parallel to the sample’s surface.

Resistance measurements were performed in-situ with a standard four probe technique [15]. We have used a constant current source to maintain a current of 0.01 mA through the film. From the dimensions of the films deposited on the substrates and the resistance measured, the electrical resistivity was calculated.

Results and Discussions

AFM Analysis

To understand the surface features and size distribution of the prepared films in the present study, we performed an analysis using atomic force microscopy. The AFM images of two films with thicknesses of 10 nm and 30 nm are presented in the three-dimensional pictures, figure 1 (a and b). Initially, an island structure for the Cr film with a thickness of 10 nm was observed, and a pyramid/columnar shape as the thickness increased to 30 nm as shown in figure 1 (a) (i) and (ii) and figure 1 (b) (i) and (ii). Furthermore, the surface becomes smooth as the thickness increased from 10 to 30 nm, as shown in figure 1 (a) (iii) and 1 (b) (iii).

Figure 1. AFM images of chromium films of different thicknesses
(a) AFM images of Cr-10 nm thickness
(b) AFM images of Cr-30 nm thickness

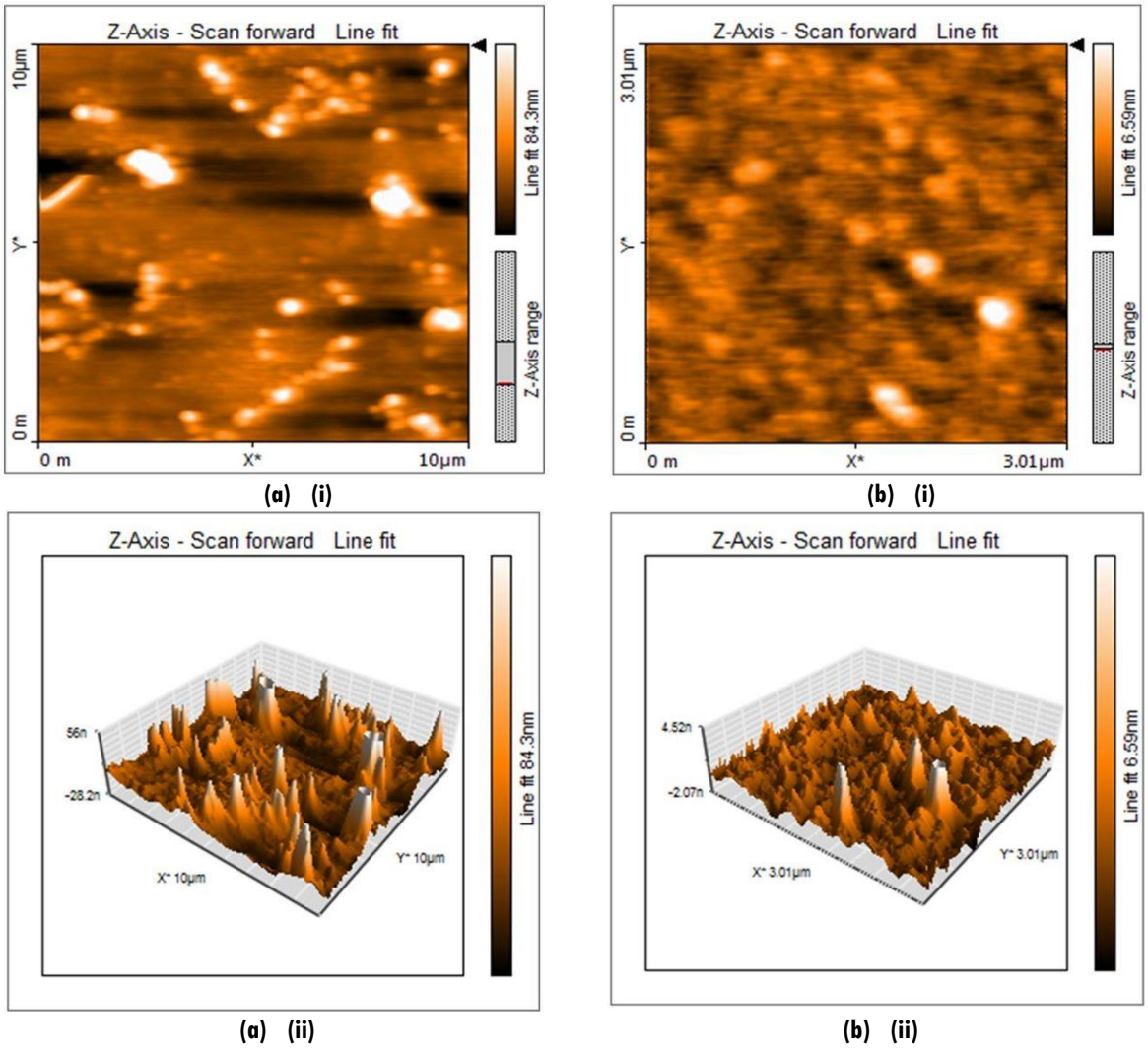

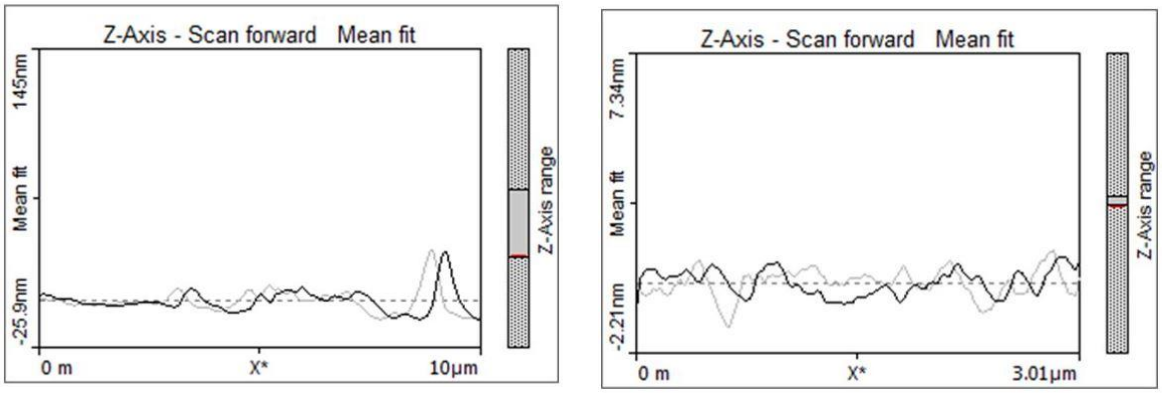

(a) (iii) **(b) (iii)**

Source: own elaboration

SEM and EDS Analysis

The most convenient and powerful tool for the microstructural studies is the use of scanning electron microscopy. SEM images of two samples of different thicknesses, 10 nm and 30 nm, along with magnifications are presented in figure 2 (a and b). Grains of different sizes with clear boundaries and non-uniform structures are depicted in figure 2 (a).

Figure 2. SEM images of chromium films of different thicknesses and magnifications
(a) SEM image of Cr (10 nm) x 10,000
(b) SEM image of Cr (30 nm) x 10,000

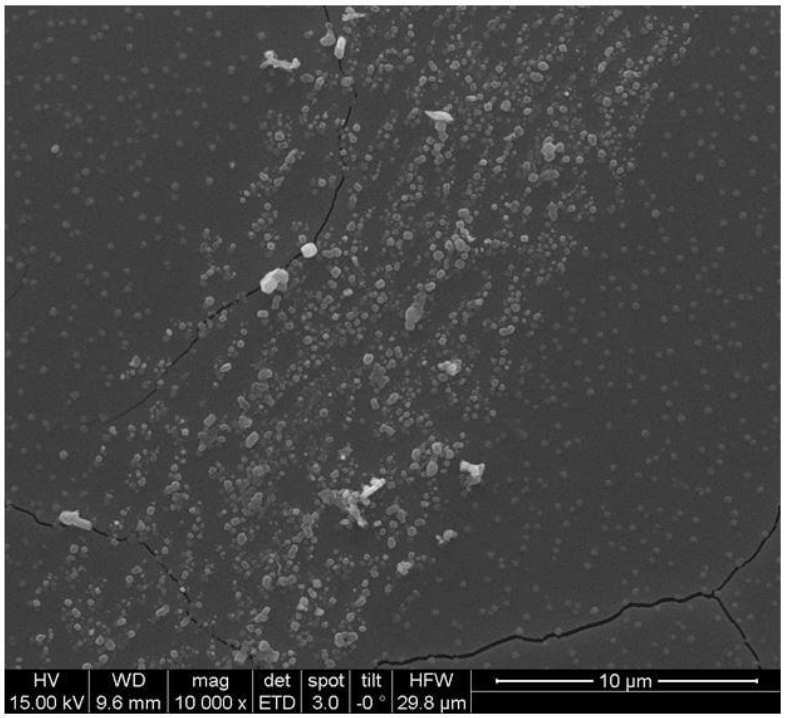

(a)

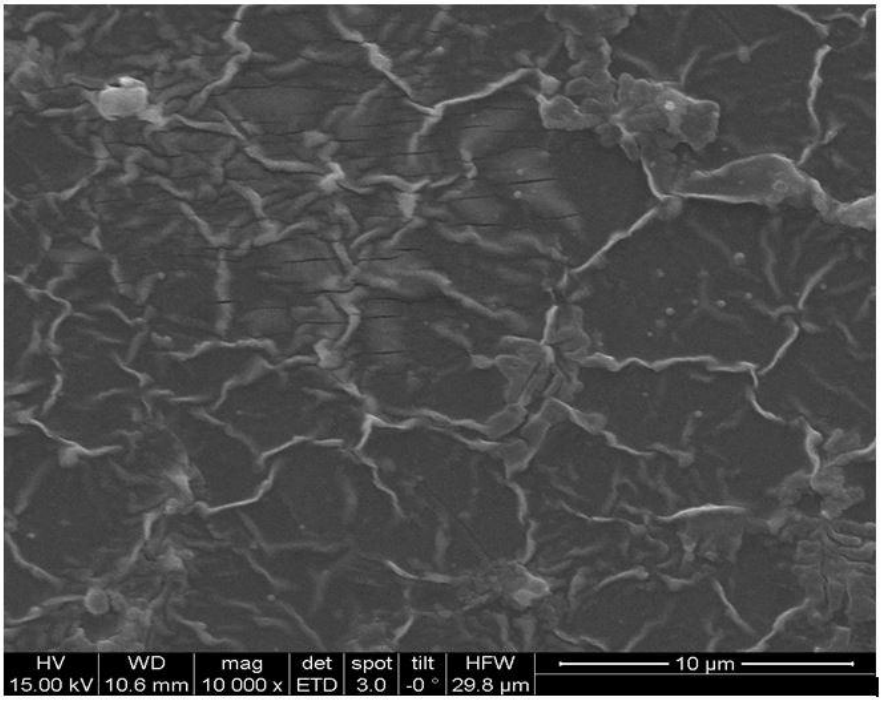

(b)
Source: own elaboration

During the initial stages of film growth, sufficient numbers of evaporated atoms hits the surface of the cooled substrate and adhere a permanently. When the substrate is exposed to incident vapor, a uniform distribution of small but highly mobile islands is observed, as shown in figure 2 (a). As condensation of atoms continues, there will be coalescence of atoms/clusters with clear boundaries, as indicated in the two-dimensional picture in figure 2 (b).

Figure 3 shows the EDS spectrum and displays the characteristic prominent peak indicating that the material utilized in the present investigation is chromium. Similar graphs and peaks have been reported by G. N. Chavan *et al.* [16] for nickel-substituted cadmium ferrites and H. L. Pushpalatha *et al.* [17] for CdS thin films.

Figure 3. EDS spectrum of chromium*

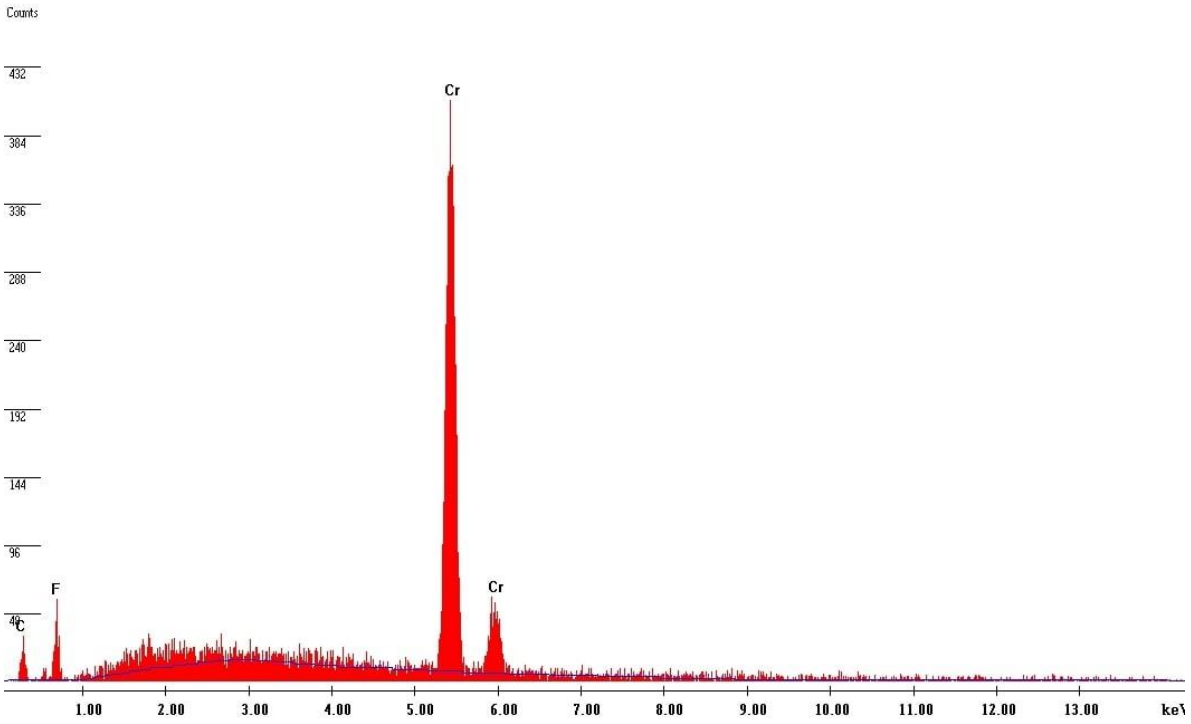

* The Y-axis shows the counts (number of X-rays received and processed by the detector), and the X-axis shows the energy level of those counts.

Source: own elaboration

Electrical Measurements and Analysis

Figure 4 shows a graph of the electrical resistivity (ρ) vs. thickness (t) for chromium films grown on soda lime glass and quartz substrates under similar environmental conditions.
It is evident from the same figure 4 that the electrical resistivity is quite large for lower-thickness films decreases for higher-thickness films and finally attains a constant value of approximately 60 x 10^{-8} Ωm and 140 x 10^{-8} Ωm for chromium films grown on soda lime glass and quartz substrates, respectively after a thickness of 30 nm.

Figure 4. Plot of electrical resistivity (ρ) against chromium film thickness (t)*

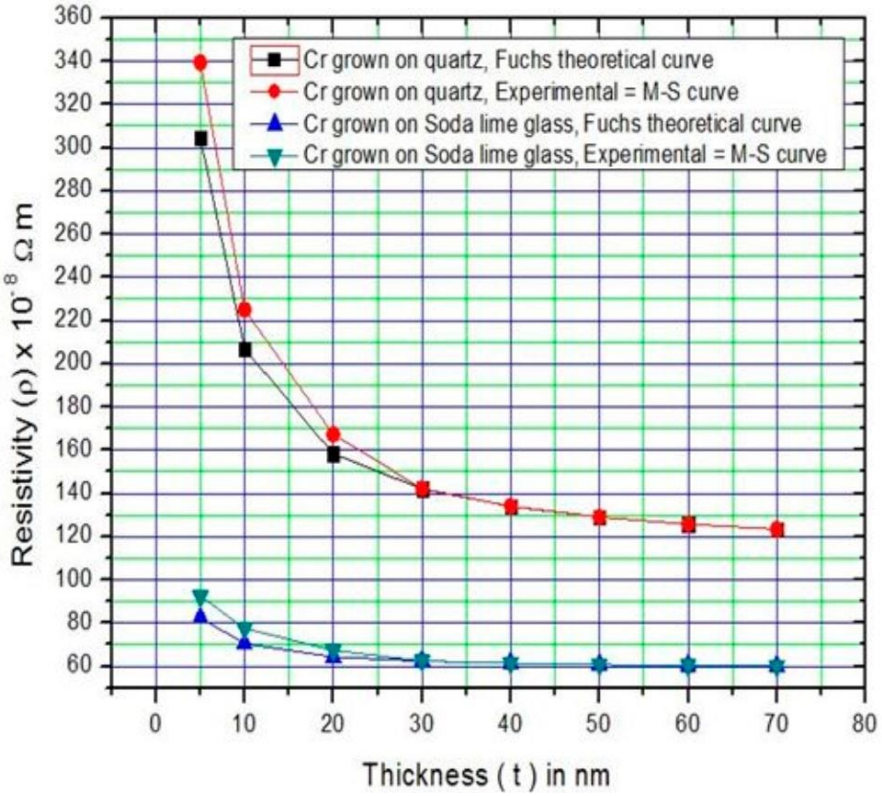

* Plot of electrical resistivity (ρ) against chromium film thickness (t) grown on soda lime glass and quartz substrates based upon Fuchs theory and our experimental data (M-S theory) (table 3).

Source: own elaboration

The uppermost (red) curve in the figure 4 is based upon the experimental results (M-S theory) of resistivity obtained in the present investigation, and the lower (black) curve is based upon Fuchs theory, for chromium films grown on quartz substrate. It is evident from this graph that the resistivity attains a constant value of approximately 140 x 10^{-8} Ωm after attaining a thickness of 30 nm.

Similarly, in the lower curve of the graph in figure 4, the upper curve (light green) represents the experimental (M-S theoretical) curve, and the lower curve (blue color) is the Fuchs theoretical curve for chromium films grown on a soda lime glass substrate. It is clear from this graph that the resistivity attains a constant value of approximately 60 x 10^{-8} Ωm after a thickness of approximately 30 nm.

Figure 5 shows (ρ x t) vs. (t) graphs, which have been plotted for chromium films deposited simultaneously on both substrates. The slopes of these graphs, according to equation 3, give ρ_0, the infinitely thick film resistivity as 58.37 x 10^{-8} Ωm and 109.6 x 10^{-8} Ωm for the films grown on soda lime glass and quartz substrates respectively; the intercepts on the (ρ x t)

axis give $\frac{3\,\rho_0\ l\,(1-p)}{8}$, as 120.44 x 10^{-17} Ωm^2 and 976.66 x 10^{-17} Ωm^2, respectively for the films grown on soda lime glass and quartz substrates, respectively.

Figure 5. Plot of (ρ x t) vs. (t)*

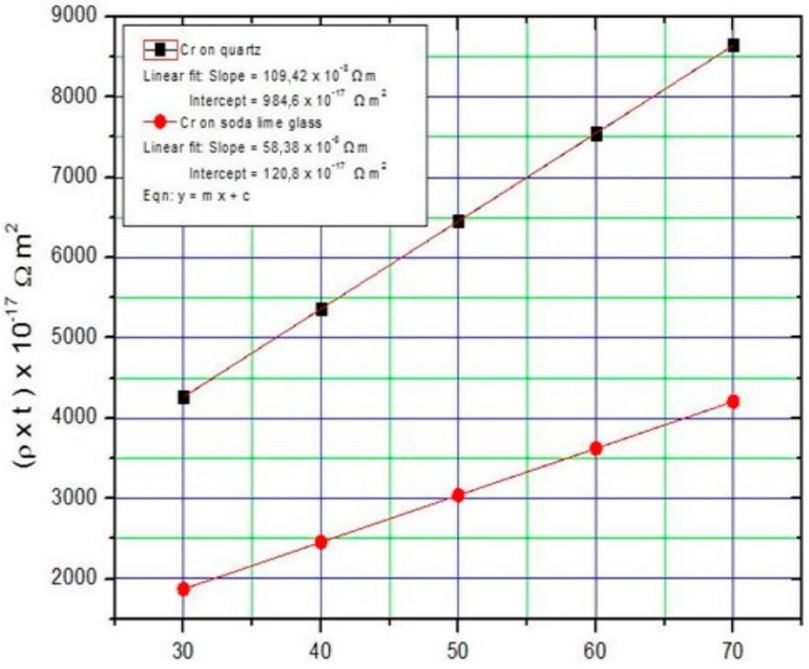

* Plot of ρ x t vs. t for chromium films grown on quartz and soda lime glass substrates for the thicknesses > 30 nm (table 4).

Source: own elaboration

We tried to fit our experimental data on the basis of F-S theory by assigning different values for *p*, the best fit was obtained for $p = 0.3$ and 0 respectively for the films grown on soda lime glass & quartz substrates, and these values are given in table 1.

Table 1. Values of ρ_0, $l(1-p)$, l and p for chromium films grown on soda-lime glass and quartz substrates

Physical parameter of chromium film	Substrate material used for growth	
	Soda lime glass	Quartz
ρ_0	58.37 x 10^{-8} Ωm	109.6 x 10^{-8} Ωm
$l\,(1-p)$	5.5 nm	23.7 nm
l	7.9 nm	23.7 nm
p	0.3	0

Source: own elaboration

We obtained good agreement between F-S theory and the experimental data for higher thicknesses (> 30 nm) for the films grown on both substrates. We obtained a mean free path of conduction electrons of 7.9 nm for $p = 0.3$ and 23.7 nm for $p = 0$ for the films grown on the soda lime glass and quartz substrates, respectively. Making use of these values, ρ_0 and

p values of *l* were calculated for the films grown on both the substrates and are listed in table 1.

The resistivity ρ_0, of infinitely thick chromium films grown on soda lime glass and quartz substrates, 58.37 x 10^{-8} Ωm and 109.6 x 10^{-8} Ωm respectively estimated from figure 5 are quite high in comparison with the bulk resistivity of chromium 12.9 x 10^{-8} Ωm [18].

Although there is perfect agreement between F-S theoretical results and our experimental curves for higher-thickness films, there is, however, some deviation from the theoretical curves for lower-thickness films. This is attributed to the fact that the F-S theory takes into account the variation in resistivity due to the size effect and disregards grain boundary scattering which is predominant in lower-thickness films.
Similar deviations between F-S theory and experimental data at lower thicknesses have also been reported for palladium [19], samarium [20], manganese [21], yttrium [22], ytterbium [23] and tin [24] films.

We tried to fit our experimental data with M-S theory. The theoretical curves based on M-S theory for chromium films grown on soda lime glass and quartz substrates are denoted as the upper curves with experimental points in figure 1 for each substrate. It is clear from the figure 1 that there is good agreement between M-S theory and the experimental data for thinner films where grain boundary scattering is predominant.

To calculate the grain boundary reflection coefficient (R'), we assumed the grain diameter to be equal to the thickness of the film, i.e., 30 nm for Cr grown on soda lime glass and quartz substrates, below which the experimental data deviate from the F-S theoretical curves. However, for higher thicknesses of chromium films (> 30 nm), the grain diameter becomes very large in comparison with the mean free path of conduction electrons, and hence, contribution to the film resistivity from the grain boundaries becomes negligible.
The difference between the resistivity from the F-S theoretical curve and the experimental data (M-S curve) gives $(\frac{3\,\alpha'\,\rho_0}{2})$. Using the values of ρ_0 and l estimated from the Fuchs theory, we obtained the value of α' and from this the constants R'_{av} (R' average) was found to be 0.090 and 0.044 for the films grown on soda lime glass and quartz substrates, respectively, as shown in the table 2. These values were used in equation 7 to obtain an M-S theoretical curve.

Table 2. Values of α', R' and R'_{av} for chromium films grown on soda-lime glass and quartz substrates at different film thicknesses (t)

	Film thickness	Cr grown on soda lime glass			Cr grown on quartz		
Sl. No.	***t* in nm**	α'	R'	R'_{av}	α'	R'	R'_{av}
1	5	0.114	0.08		0.211	0.042	
2	10	0.08	0.09	0.09	0.108	0.045	0.044
3	20	0.034	0.09		0.048	0.045	

Source: own elaboration

The growth and structure of evaporated films are greatly affected by the nature of the substrate, smoothness/roughness and the binding force between the substrates and evaporated atoms. An increase in the binding force between the substrate and evaporated atoms, usually, decreases the surface mobility of evaporated atoms and hence increases the population of critical nuclei. This, in turn, enhances film adhesion. Therefore, the film resistivity may be considerably reduced.

The theoretical curves based on M-S theory are shown in figure 4. It is clear from this figure that there is good agreement between M-S theory and our experimental data for chromium films coated on both substrates for thinner films where grain boundary scattering is predominant [25].

The average grain boundary reflection coefficient R'_{av} for Cr coated on soda lime glass as given in table 2, appears to be approximately double the value for Cr coated on quartz substrates. It is observed that the M-S equation reproduces the experimental observation well with $R'_{av} = 0.090$ and p = 0.3 and $R'_{av} = 0.044$ and $p = 0$ for chromium deposited on soda lime glass and quartz substrates, respectively, which indicates that the contribution from grain boundary scattering should be substantial. Naturally, this leads to the enhancement of the conduction electron mean free path of chromium coated on quartz compared to that of chromium coated on soda lime glass as presented in the table 1.

Conclusions

The AFM observations indicate that the Cr grains of different sizes are formed at the beginning of film formation and scattered on the surface of the substrate. Furthermore, on the surface of the substrate, with increased film thickness, pyramid/columnar-like structures are observed. With a further increase in film thickness, the island structure is modified to become a semicontinuous structure with clear boundaries. Investigation of film structure by SEM revealed that the films consist of grains of relatively pure chromium of different sizes, and it is concluded that the grain size which depends upon deposition conditions, which is an important factor that determines the structural properties of the films. EDS analysis of the films were carried out, and it was been confirmed that the material used in the present investigation is chromium.

F-S theory considers only the size effect, avoiding grain boundary scattering. The grain boundary scattering mechanism is predominant in thin films and is taken into account by M-S theory. Our experimental curves fit well with the M-S theoretical curves over the entire range of film thicknesses. We calculated the values of ρ_0, ρ, p, α', R' and l for chromium films grown on soda lime glass and quartz substrates.

These values depend on the nature of the binding force between chromium and the substrate material. Hence, the thickness and material of the substrate will have an appreciable effect on the parameters like ρ_0, ρ, p, α', R' and l for chromium. It is predicted

that the films of particular characteristic for specific application could be grown by selecting suitable deposition parameters or suitable combinations of deposition parameters.

Acknowledgements

One of the authors, Lingappa A. Udachan, is very thankful to Dr. B. G. Hegde, Professor, Rani Channamma University, Belagavi, Karnataka, India for constant support and encouragement.

References

[1] M. A. Angadi and L. A. Udachan, "The effect of substrate temperature on the electrical properties of thin chromium films," *J. Mater. Sci.*, vol. 16, no. 5, pp. 1412–1415, 1981, https://doi.org/10.1007/BF01033860

[2] S. J. Ikhmayies, N. M. Abu El-Haija, and N. Ahmad-BitarRiyad, "Electrical and optical properties of ZnO:Al thin films prepared by the spray pyrolysis technique," *Physica Scripta*, vol. 81, no. 1, 015703, 2010. Available: https://iopscience.iop.org/article/10.1088/0031-8949/81/01/015703.

[3] D. J. Ranir, A. Guru Sampath Kumar, and T. Subba Rao, "Substrate temperature-dependent physical properties of nanocrystalline zirconium titanate tin films," *J. Coatings Techn. Res.*, vol. 14, no. 5, pp. 971–980, 2017.

[4] S. A. Jassim, A. A. R. A. Zumaila, and G. A. A. Waly, "Influence of substrate temperature on the structural, optical and electrical properties of CdS thin films deposited by thermal evaporation," *Results Phys.*, vol. 3, pp. 173–178, 2013. Available: https://doi.org/10.1016/j.rinp.2013.08.003

[5] F. A. Mir, M. Ikram, and Ravi Kumar, "Impact of substrate on some physical properties of PrFe0.5Ni0.5O3 thin films," *Solid State Sci.*, vol. 13, no. 11, pp. 1994–1999, 2011. Available: https://doi.org/10.1016/j.solidstatesciences.2011.09.001

[6] M. Cao *et al.*, "Influence of substrates on the structural and optical properties of ammonia-free chemically deposited CdS films," *J. Alloys Compounds*, vol. 530, pp. 81–84, 2012. Available: https://doi.org/10.1016/j.jallcom.2012.03.054

[7] J. K. Ros *et al.*, "The effect of substrate roughness on the surface structure of TiO2, SiO2, and doped thin films prepared by the sol-gel method," *Acta Bioeng. Biomech.*, vol. 11, no. 2, pp. 1–9, 2009. Available: http://www.actabio.pwr.wroc.pl/Vol11No2/3.pdf

[8] M. A. Angadi and L. A. Udachan, "The effect of the deposition rate on the electrical resistivity of thin tin films," *Thin Solid Films*, vol. 78, no. 3, pp. 299–302, 1981. Available: https://doi.org/10.1016/0040-6090(89)90597-X

[9] M. A. Angadi and L. A. Udachan, "Influence of DC electric field on sheet resistance of thin tin and chromium films," *J. Phys. D Appl. Phys.*, vol. 14, no. 5, pp. L81, 1981, https://iopscience.iop.org/issue/0022-3727/14/5

[10] Ch. Kittel, *Introduction to Solid State Physics*. New Delhi: Wiley India Pvt. Ltd., 2010.

[11] K. Fuchs, "Electrical resistance in thin metal films," *Proc. Cambr. Philo. Soc.*, vol. 34, no. 1, pp. 100–193, 1938.

[12] D. C. Larson, *Physics of Thin Films*, vol. 6, M. H. Francombe and R. W. Hoffmann, Eds. New York, NY, USA: Academic Press, 1971.

[13] E. H. Sondheimer, "The influence of a transverse magnetic field on the conductivity of thin metallic films," *Phys. Rev.*, vol. 80, no. 3, pp. 401–406, 1950. doi:10.1103/PhysRev.80.401

[14] A. F. Mayadas and M. Shatzkes, "Electrical-resistivity model for polycrystalline films: The case of arbitrary reflection at external surfaces," *Phys. Rev. B*, vol. 1, no. 4, pp. 1382–1389, 1970. Available: https://doi.org/10.1103/physrevb.1.1382

[15] M. K. Thakur *et al.*, "Effect of substrate on the structural and electrical properties of Mo thin films," *Adv. Mater. Lett.*, vol. 7, no. 7, pp. 525–528, 2016. doi: 10.5185/amlett.2016.5965

[16] G. N. Chavan, P. B. Belavi, L. R. Naik, V. L. Mathe, and R. K. Kotnala, "Resistivity and grain size dependent magnetoelectric effect in (Y) Ni0.85Cd0.1Cu0.05Fe2O4 + (1-Y) Batio3 ME composites," *Int. J. Sci. Techn. Res.*, vol. 2, no. 12, pp. 298–306, 2013. Available: http://www.ijstr.org/final-print/dec2013/Resistivity-And-Grain-Size-Dependent-Magnetoelectric-Effect-In-Y-Ni0.85cd0.1cu0.05fe2o4-+-1-y-Batio3-Me-Composites.pdf

[17] H. L. Pushpalatha, S. Bellappa, T. R. Narayanaswamy, and R. Ganesha, "Structural and optical properties of CdS thin film obtained by chemical bath deposition and effect of annealing," *Indian J. Appl. Phys.*, vol. 52, no. 08, pp. 545–549, 2014. Available: https://pdfs.semanticscholar.org/96a0/4cdc5cae8ec4dc77936869eedc99cdfac867.pdf

[18] *Handbook of Physics and Chemistry*, 54 ed. Cleveland, Ohio, USA: Chemical Rubber Company Press.

[19] S. M. Shivaprasad, L. A. Udachan, and M. A. Angadi, "Electrical resistivity of thin palladium films," *Phys. Lett.*, vol. 78A, no. 2, pp. 187–188, 1980. Available: https://doi.org/10.1016/0375-9601(80)90693-3

[20] J. Kumar and O. N. Srivastava, "Electrical resistivity of thin films of samarium," *Thin Solid Films*, vol. 13, no. 2, pp. S29–S33, 1972. Available: https://doi.org/10.1016/0040-6090(72)90323-9

[21] S. M. Shivaprasad, M. A. Angadi, and L. A. Udachan, "Temperature coefficient of resistance of thin manganese films," *Thin Solid Films*, vol 71, no. 1, pp. L1–L4, 1980. Available: https://doi.org/10.1016/0040-6090(80)90170-4

[22] P. V. Ashrit, S. M. Shivaprasad, and M. A. Angadi, "Electrical resistivity of thin Yttrium films," *Thin Solid Films*, vol. 72, pp. L5–L6, 1980.

[23] P. V. Ashrit and M. A. Angadi, "Electrical properties of thin ytterbium films," *Phys. Status Solid.*, vol. 63, p. K77, 1981. doi: 10.1002/pssa.2210630168

[24] M. A. Angadi and L. A. Udachan, "The effect of the deposition rate on the electrical resistivity of thin tin films," *Thin Solid Films*, vol. 78, pp. 299–302, 1980. Available: https://doi.org/10.1016/0040-6090(89)90597-X

[25] S. K. Bandyopadhyay and A. K. Pal, "The effect of grain boundary scattering on the electron transport of aluminium films," *J. Phys. D Appl. Phys.*, vol. 12, no. 6, pp. 953–960, 1979. Available: https://doi.org/10.1088/0022-3727/12/6/018

Appendices

Figure 4 plot of electrical resistivity (ρ) against chromium film thickness (t) grown on soda lime glass and quartz substrates based upon Fuchs theory and our experimental (M-S theory) results.

Table 3. Plot of electrical resistivity (ρ) against chromium film thickness (t)

		Chromium grown on quartz		Chromium grown on soda lime glass	
Sl. No.	**Thickness (t) in nm**	**Resistivity (ρ_F) due to Fuchs x 10^{-8} Ωm**	**Resistivity (ρ_{exp}) (experimental) x 10^{-8} Ωm**	**Resistivity (ρ_F) due to Fuchs x 10^{-8} Ωm**	**Resistivity (ρ_{exp}) (experimental) x 10^{-8} Ωm**
1	5	304.44	339.44	82.5	92.5
2	10	207	225	70.5	77.5
3	20	158.3	167.3	64.4	67.4
4	30	142.1	142.2	62.4	62.4
5	40	134	134.1	61.4	61.4
6	50	129.1	129.1	60.8	60.8
7	60	125.8	125.8	60.4	60.4
8	70	123.5	123.5	60.1	60.1

Source: own elaboration

Figure 5 shows the (ρ x t) vs. film thickness (t) for Cr films grown on soda lime glass and quartz substrates (t > 30 nm).

Table 4. (ρ x t) vs. film thickness (t)

		Chromium grown on quartz	Chromium grown on soda lime glass
Sl. No.	**Thickness (t) in nm**	**(ρ x t) x 10^{-17} in Ωm^2**	**(ρ x t) x 10^{-17} in Ωm^2**
1	30	4266	1872
2	40	5364	2456
3	50	6455	3040
4	60	7548	3624
5	70	8645	4207

Source: own elaboration